

Original Article

Absorption mechanism of DHP107, an oral paclitaxel formulation that forms a hydrated lipidic sponge phase

Yura JANG^{1, 2}, Hye Jin CHUNG³, Jung Wan HONG¹, Cheol-Won YUN², Hesson CHUNG^{1, *}

¹Center for Neuro-Medicine, Korea Institute of Science and Technology, 5 Hwarang-ro 14-gil, Seongbuk-gu, Seoul 02792, Republic of Korea; ²School of Life Sciences and Biotechnology, Korea University, 145 Anam-ro, Seongbuk-gu, Seoul 02841, Republic of Korea; ³College of Pharmacy and Research Institute of Pharmaceutical Sciences, Gyeongsang National University, 501 Jinju-daero, Jinju, Gyeongnam 52828, Republic of Korea

Abstract

Paclitaxel is a most widely used anticancer drug with low oral bioavailability, thus it is currently administered via intravenous infusion. DHP107 is a lipid-based paclitaxel formulation that can be administered as an oral solution. In this study, we investigated the mechanism of paclitaxel absorption after oral administration of DHP107 in mice and rats by changing the dosing interval, and evaluated the influence of bile excretion. DHP107 was orally administered to mice at various dosing intervals (2, 4, 8, 12, 24 h) to examine how residual DHP107 affected paclitaxel absorption during subsequent administration. Studies with small-angle X-ray diffraction (SAXS) and cryo-transmission electron microscopy (cryo-TEM) showed that DHP107 formed a lipidic sponge phase after hydration. The AUC values after the second dose were smaller than those after the first dose, which was correlated to the induction of expression of P-gp and CYP in the livers and small intestines from 2 h to 7 d after the first dose. The smaller AUC value observed after the second dose was also attributed to the intestinal adhesion of residual formulation. The adhered DHP107 may have been removed by ingested food, thus resulting in a higher AUC. In *ex vivo* and *in vivo* mucoadhesion studies, the formulation adhered to the villi for up to 24 h, and the amount of DHP107 that adhered was approximately half that of monoolein. The paclitaxel absorption after administration of DHP107 was not affected by bile in the cholecystectomy mice. The dosing interval and food intake affect the oral absorption of paclitaxel from DHP107, which forms a mucoadhesive sponge phase after hydration. Bile excretion does not affect the absorption of paclitaxel from DHP107 *in vivo*.

Keywords: paclitaxel; DHP107; oral formulation; drug absorption; sponge phase; P-gp; CYP; mucoadhesiveness; dosing regimen

Acta Pharmacologica Sinica (2017) 38: 133–145; doi: 10.1038/aps.2016.105; published online Nov 21 2016

Introduction

DHP107 is a single-agent oral paclitaxel formulation prepared as a semi-solid wax that melts at approximately 30°C and is composed of monoolein, tricaprylin, polysorbate 80, and 1% (*w/v*) paclitaxel^[1, 2]. DHP107 is an oily liquid at body temperature that can be administered as an oral solution. We have previously designed DHP107 to be mucoadhesive in the gastrointestinal tract to facilitate adhesion to mucosal cells in the stomach and upper intestine^[1-7]. Paclitaxel is one of the most widely used drugs used for the treatment of various cancers, such as breast, lung, and ovarian cancers^[8]. Paclitaxel is currently administered as an intravenous infusion, owing to its

low oral bioavailability. Several attempts have been made to develop oral paclitaxel formulations; however, there are currently no oral paclitaxel-based products available on the market^[8-19].

In animal studies, the relative oral bioavailability of DHP107 at a dose of 50 mg/kg has been shown to be approximately 23% that of intravenous injection of paclitaxel (Taxol[®]) at a dose of 10 mg/kg^[2]. In addition, the antitumoral effects of orally administered DHP107 (50 mg/kg) are comparable to those of intravenously injected Taxol[®] (10 mg/kg) in mice inoculated with lung, breast, and ovarian cancer cell lines^[1, 2, 20]. In a previous first-in-human study, a single escalating dose of oral DHP107 was shown to be safe and feasible, with no dose-limiting toxicity when administered at up to 600 mg/m² in patients with advanced solid tumors^[21, 22]. In a phase I study, the recommended oral dose of DHP107 has been reported to

*To whom correspondence should be addressed.

E-mail heschung@kist.re.kr

Received 2016-06-30 Accepted 2016-08-31

be 200 mg/m² twice daily (b.i.d.) in patients with metastatic solid tumors^[22, 23]. DHP107 has also been shown in phase II studies to have antitumoral effects with no treatment-related deaths in patients with advanced gastric cancer^[23]. In a phase III clinical study, DHP107 was administered b.i.d. at 10-h intervals once per week at 200 mg/m² and was found to be non-inferior to Taxol[®] in terms of progression-free survival when administered as a second-line treatment for advanced gastric cancer^[24].

Such b.i.d. dosing has also been attempted in one of the first clinical trials of another oral paclitaxel formulation^[25–27] and has been reported to be effective when oral paclitaxel (Paxene[®] or Paxoral[®]) is administered with cyclosporine A^[25–27]. Repeated dosing studies of DHP107 have also been performed in animal models, and DHP107 has been used in metronomic therapy in a mouse model of ovarian cancer^[20]. DHP107 orally administered to mice on a metronomic schedule (25 mg/kg, twice a week) has been found to have significantly greater antitumor effects than those resulting from a high-dose regimen (50 mg/kg, weekly). Thus, regular, long-term, low-dose administration of the drug is more effective than short-term, high-dose administration. The authors have concluded that longer exposure to paclitaxel as DHP107 effectively reduces tumor growth by decreasing the recovery time of the damaged tumor^[20, 25]. This result is somewhat surprising because the absorption of paclitaxel is known to decrease after repeated dosing, owing to the induction of P-glycoprotein (P-gp) and cytochrome P450 (CYP).

In this study, we performed a pharmacokinetic study in mice by changing the dosing interval of orally administered DHP107 to determine how residual DHP107 in the gastrointestinal tract changes the absorption of paclitaxel during subsequent administration, and to obtain insight into the absorption mechanisms and properties of the DHP107 formulation. We also studied the physicochemical characteristics of DHP107 by electron microscopy and X-ray diffraction to determine the mucoadhesive properties of the formulation. Mucoadhesiveness was evaluated by performing *ex vivo* everted sac studies and observing the intestinal lumen under a microscope. Finally, the effects of bile on the absorption of DHP107 were studied.

Materials and methods

Materials

DHP107 (10 mg/mL), provided by Daehwa Pharmaceutical (Seoul, Korea), was composed of 1% (*w/w*) paclitaxel, 55% monoolein, 27.5% tricaprilyn, and 16.5% polysorbate 80. Paclitaxel was obtained from Samyang Genex (99.7%, Seoul, Korea). Distilled monoolein (RYLO[™] MG 19, >90% pure) was purchased from Danisco Ingredients (Copenhagen, Denmark). Taxol[®] was obtained from Corden Pharma Latina SPA (Sermometa LT, Italy). Polysorbate 80, tricaprilyn, polysorbate 20, polyethylene glycol 400 (PEG 400), sucrose, cremophor EL, oil red O, Nile red, monobasic potassium phosphate, pancreatin, sodium hydroxide, chloroform, formic acid, and docetaxel were obtained from Sigma-Aldrich (St Louis, MO, USA).

Ethyl alcohol was obtained from Daejung Chemicals & Metals Co, Ltd (Siheung, Korea). Tris-HCl (1 mol/L, pH 7.4) was purchased from Bioneer Co (Daejeon, Korea). High-performance liquid chromatography (HPLC)-grade acetonitrile, methyl alcohol, and methyl *tert*-butyl ether were purchased from JT Baker (Phillipsburg, NJ, USA). To prepare DHP107, paclitaxel and tricaprilyn were dissolved completely in excess methylene chloride. After complete evaporation of methylene chloride by vacuum evaporation (BUCHI Rotavapor R-200, Germany) at 40 °C for 1 h, monoolein and polysorbate 80 were added and mixed thoroughly by sonication for 30 s. The residual solvent was removed by vacuum evaporation to produce DHP107. A paclitaxel-free formulation of DHP107 (F109) was prepared by mixing monoolein, tricaprilyn, and polysorbate 80 at 1:0.5:0.3 (*v/v/v*) at 40 °C.

Differential scanning calorimetry

Differential scanning calorimetry (DSC 821e, Mettler Toledo, Columbus, OH, USA; equipped with an Intracooler, Haake EK90/MT, Haake, Denmark) was performed for dry and hydrated F109 and DHP107 at a heating scan rate of 2 °C/min. The hydrated samples contained 50% (*v/v*) water. The thermograms were normalized by the weight of F09 and DHP107 in the samples for comparison.

Small-angle X-ray diffraction

F109 and DHP107 samples were prepared at various hydrations in 1-mm quartz capillaries (Charles Supper Co, Natick, MA, USA). Small-angle X-ray diffraction (SAXS) patterns were collected for 6 h at room temperature using a rotating anode X-ray diffractometer (Rigaku D/MAX-2500; Rigaku, Tokyo, Japan) operated at 50 kV and 100 mA at an incident wavelength of 1.54 Å (Cu K α). Diffraction patterns were collected in the 2 θ range from 0.2 to 5° using an image plate system (Rigaku) at a sample-to-detector distance of 30 cm.

Cryo-transmission electron microscopy (cryo-TEM)

Hydrated F109 and DHP107 samples were prepared in 25% (*v/v*) water. The sponge phase sample was prepared as a control by mixing PEG 400, monoolein, and 100 mmol/L Tris-HCl buffer (4:3:3, *v:v:v*) as previously described^[28]. Micrographs of the samples were observed by electron tomography using a cryo-TEM (G2 F20; Tecnai, Hillsboro, OR, USA) operated at 200 kV and equipped with a scanning transmission electron microscope (STEM) and a 2k CCD (charge-coupled device) camera in high-angle annular dark-field mode.

Animal handling

Seven-week-old female BALB/c mice (17–19 g) and Sprague-Dawley rats (160–170 g) were purchased from Nara Biotech (Seoul, Korea). The mice and rats were housed in group cages (26 cm×20 cm×13 cm for mice and 42 cm×26 cm×18 cm for rats; Jeung Do Bio & Plant Co, Seoul, Korea) with autoclaved corncob bedding (Harlan Teklad, Madison, WI, USA) under a 12:12 h light/dark cycle (lights on at 08:00 h). The rodents were fed irradiated pelleted chow (Harlan Teklad) *ad libitum*

and had free access to sterilized drinking water. Euthanasia was performed with carbon dioxide. All animal care and handling procedures were performed according to the guidelines of the Animal Care and Use Committee of Korea Institute of Science and Technology (protocol number: 2015-002).

Oral administration of F109 and DHP107 under fasted and fed conditions in mice

DHP107 was liquefied by warming to 36°C and was administered as an oral solution to mice at a single dose of 50 mg/kg under fasted (overnight) and fed conditions ($n=5-20$ /time point). Blood was collected by cardiac puncture while mice were anesthetized with ether at 0.5, 1, 2, 4, 8, 12, and 24 h after administration of DHP107. In additional mouse groups, DHP107 was administered twice at dosing intervals of 2, 4, 8, 24, 48, and 96 h ($n=5$ /time point, 50 mg/kg each). To evaluate whether pre-administration of F109 influenced the absorption of the second dose of DHP107, 5 mL/kg F109 was administered as the first dose instead of DHP107 to additional groups of fasted and fed mice ($n=5$ /time point). DHP107 and F109 were melted by warming to body temperature before feeding, as described previously^[2]. Blood was collected at 0.5, 1, 2, 4, 8, 12, and 24 h after the second dose of DHP107 via cardiac puncture while mice were anesthetized with ether. Plasma samples were separated by centrifugation. All samples were stored at -70°C until analysis by liquid chromatography-tandem mass spectrometry (LC-MS/MS).

Western blotting

DHP107 was administered to mice at a dose of 50 mg/kg under fasted conditions ($n=3$ /time point). At 2, 4, 8, 12, and 24 h and 4 and 7 d after DHP107 administration, mice were sacrificed via cardiac puncture while they were under anesthesia with ether, and the livers and small intestines were immediately harvested. Untreated mice were used as controls (0 h). Western blotting was performed as described previously^[29]. The livers and small intestines were washed with ice-cold phosphate-buffered saline (PBS) containing a complete EDTA-free protease inhibitor cocktail (Roche Diagnostics, Risch-Rotkreuz, Switzerland). For Western blot analysis, tissue samples in 50 mmol/L Tris-HCl (pH 7.4) containing 250 mmol/L sucrose, protease inhibitor, and phosSTOP phosphatase inhibitor cocktail (Roche Diagnostics) were homogenized on ice (Ultra-Turrax T25 basic; IKA Labortechnik, Staufen, Germany) and centrifuged at 5000×g for 10 min at 4°C. The debris was discarded, and supernatants were centrifuged again at 100 000×g for 30 min at 4°C. The resulting pellets were resuspended in 50 mmol/L Tris-HCl containing protease and phosphatase inhibitors by brief homogenization on ice, and the samples were stored at -70°C until analysis. Protein concentrations were determined using a BCA protein assay kit (Pierce, Rockford, IL, USA) with bovine serum albumin as the standard.

Tissue extracts (30 µg/lane) were loaded onto 10% sodium dodecyl sulfate (SDS) polyacrylamide gels and separated by SDS-polyacrylamide gel electrophoresis (SDS-PAGE) at 80 V

for 15 min followed by 150 V for 30 min. Next, the proteins in the gels were transferred to polyvinylidene fluoride (PVDF) membranes (Bio-Rad Laboratories, Hercules, CA, USA) at 400 mA for 1 h. The membranes were incubated with blocking buffer containing 5% (*w/v*) skim milk and 0.1% (*v/v*) polysorbate 20 in Tris-buffered saline (TBS) for 1 h at room temperature. P-glycoprotein (P-gp) and cytochrome P450 (CYP3A4 and CYP2C8) were detected by incubation with anti-P-gp (Calbiochem, San Diego, CA, USA), anti-CYP3A4 (Cell Signaling Technology, Beverly, MA, USA), and anti-CYP2C8 (Chemicon International, Temecula, CA, USA) antibodies, respectively, overnight at 4°C. Tubulin expression was detected with anti- α -tubulin antibodies (Santa Cruz Biotechnology, Santa Cruz, CA, USA) as a control for all samples. The membranes were washed three times with washing buffer containing 0.1% (*v/v*) polysorbate 20 in TBS and incubated for 1 h at room temperature with horseradish peroxidase-conjugated anti-mouse or anti-rabbit antibodies (Santa Cruz Biotechnology). Bands were detected by chemiluminescence using a ChemiDoc MP imaging system (Bio-Rad Laboratories).

Bile collection and sampling in rats

For bile collection, the rats were anesthetized by intramuscular injection of a 2:1 mixture of Zoletil® (Virbac Laboratories, Carros, France) and Rompun® (Bayer Korea, Anshan, Korea) at a dose of 0.5 mL/kg. The bile was drained from the rats through the bile duct by inserting polyethylene tubing as a single cannula. The cannula was pulled out toward the back of the neck through the skin. A harness was placed on each rat, and the cannula was embedded in the harness to prevent displacement. The rats were subsequently placed in cages for 24-h bile collection^[30]. The collected rat bile was stored at -70°C until use.

For pharmacokinetic studies, the rats were cannulated under anesthesia: a catheter was inserted (Intramedic PE-50) into the jugular vein of each rat, and the rats were allowed to recover for 1 d before pharmacokinetic studies^[31]. Before dosing, the rats were fasted overnight, and distilled-deionized water (control) or bile collected from other rats was orally administered at a dose of 5 mL/kg at 1 min after oral administration of 25 mg/kg DHP107 ($n=10$ /group). Blood was collected at 0.5, 1, 2, 4, 8, 12, and 24 h after administration of DHP107. Plasma samples were separated by centrifugation, and all samples were stored at -70°C until LC-MS/MS analysis.

Cholecystectomy and sampling in mice

The mice were anesthetized by intraperitoneal injection of a Zoletil® and Rompun® mixture (2:1, *v/v*) at a dose of 1 mL/kg. The hair on the chests and abdomens of the mice was shaved with electric clippers, and the peritoneal cavity was opened. To establish the cholecystectomy model, the cystic ducts were double ligated with a 6-0 silk suture and cut between the ligatures. In sham-operated control mice, the peritoneal cavity was opened and exposed, but the cystic duct was neither ligated nor removed^[32].

After ensuring that the mice continued to gain weight nor-

mally, we orally administered DHP107 to the sham-operated and cholecystectomized mice at a dose of 50 mg/kg under fasted conditions ($n=5$ /time point). Blood was collected at 0.5, 1, 2, 4, 8, 12, and 24 h after administration of DHP107 by cardiac puncture while the mice were anesthetized with ether. Plasma samples were stored at -70°C until LC-MS/MS analysis.

Measurement of paclitaxel in the plasma and pharmacokinetic analysis

To determine the paclitaxel concentration in the plasma, a 50 μL plasma sample was mixed with 50 μL of internal standard (docetaxel; 0.1 $\mu\text{g}/\text{mL}$ in acetonitrile) and 1 mL methyl *tert*-butyl ether. The tubes were vortexed and centrifuged for 10 min at $10000\times g$ at 4°C . The organic phase layer was transferred to a new tube and evaporated at 35°C under a gentle stream of nitrogen. The residue was reconstituted in the mobile phase, as described below. The reconstituted solutions were vortexed and centrifuged for 5 min at $10000\times g$ at 4°C . The supernatant was transferred to an HPLC vial for analysis^[7].

LC-MS/MS analysis was performed using an Agilent 1260 HPLC system (Agilent Technologies, Santa Clara, CA, USA) coupled to an Agilent 6460 triple quadrupole mass spectrometer (Agilent Technologies) equipped with an electrospray ionization source. The mobile phase consisted of 0.1% formic acid and acetonitrile (4:6, *v/v*), and the isocratic elution method was used. The analytical column was an Agilent Poroshell 120 EC-C 18 column (2.7 μm , 3.0 mm \times 50 mm; Agilent Technologies). Paclitaxel and docetaxel were eluted at approximately 1.8 and 1.7 min, respectively, at a flow rate of 0.3 mL/min. The total run time was 3 min, and the injection volume was 10 μL . Ion detection was performed in multiple reaction monitoring (MRM) mode, and the following precursor-to-product ions were monitored: m/z 854.2 \rightarrow 569.2 for paclitaxel and m/z 808.3 \rightarrow 527.2 for the internal standard. Data acquisition was acquired using an Agilent Mass Hunter Workstation software (Agilent Technologies).

For bioanalytical method validation, quality control samples were analyzed five times per day and once per day for 5 d for three concentrations of paclitaxel in the plasma. Calibration curves were constructed using weighted regression ($1/x^2$) by plotting the peak area ratio of paclitaxel to the ratio of the internal standard and concentration^[33]. The accuracy varied from 85.3% to 111.7% in mouse plasma and 89.5% to 113.5% in rat plasma. The intra-day and inter-day precisions (coefficients of variation) did not exceed 7.1% in mouse plasma and 9.6% in rat plasma.

The mean and standard error of the mean at each time point were calculated, and pharmacokinetic parameters were determined from the mean concentration data via a noncompartmental analysis using the WinNonlin program (Pharsight Corporation, Mountain View, CA, USA).

Everted sac experiment

The everted sac experiment was performed by using the upper

small intestine of the mice to evaluate the mucoadhesiveness of DHP107, as described previously^[34]. The mice were sacrificed, and the jejunum portions of small intestines were excised and immersed in ice-cold PBS. The collected intestines were perfused with ice-cold PBS to remove intestinal content and then everted using a blunt needle. The content of the everted intestines was washed out with ice-cold PBS. Each of the intestinal segments was cut to lengths of 3 cm, and a plastic piston of the pipette tip (2 mm in diameter; CP250, Microman, Gilson) was inserted to straighten the segments. Ligatures were made at each end to close the segments. Oil red O, a colorimetric probe, was mixed with F109, cremophor EL:ethyl alcohol (1:1, *v/v*; Taxol[®] formulation), monoolein, tricaprilyn, polysorbate 80, monoolein/polysorbate 80 (1:0.3, *v/v*), tricaprilyn/polysorbate 80 (0.5:0.3, *v/v*), and monoolein/tricaprilyn (1:0.5, *v/v*) at 5 mg/mL. The everted sacs were immersed in 3 mL of the above oil preparations containing oil red O in 15-mL conical tubes ($n=6$ /group). After incubation at 37°C for 10 min in a shaking water bath, the samples were transferred to new tubes containing 10 mL of simulated intestinal fluid prepared with 0.69% (*w/v*) potassium dihydrogen phosphate, 1% (*w/v*) pancreatin, and 1.9% (*w/v*) sodium hydroxide solution (0.2 mol/L) at pH 7.5^[35] and were incubated at 37°C for 30 min in a shaking water bath. Each sac was transferred to a new tube and freeze-dried. Oil red O was extracted by addition of 3 mL of organic extraction solvent (chloroform:methyl alcohol=1:1, *v/v*), vortexing, and quantification at 518 nm using a microplate reader (FlexStation 3; Molecular Devices, Sunnyvale, CA, USA).

Mucoadhesiveness of DHP107 *in vivo*

F109 was administered to mice at a dose of 5 mL/kg under fasted and fed conditions ($n=3$ /group). Nile red, a colorimetric probe, was dissolved at 0.2 mg/mL in F109. Mice were sacrificed at 2 and 24 h after F109 administration by cardiac puncture under anesthesia with ether, and the jejunum portions of the small intestines were harvested and collected. The intestines were perfused with PBS to remove the intestinal content, including loosely attached F109 formulations. Rings of intestine samples (0.1 mm thickness) were mounted on glass slides^[2] and observed under a microscope (Olympus BX51 microscope; Olympus Co, Tokyo, Japan) with a CCD camera (Olympus DP70 Digital Microscope Camera). Fluorescence images of the intestinal lumens were visualized using a filter (excitation: 510–550 nm and emission: 590 nm).

Statistical analysis

All data are presented as the mean \pm standard deviation. Two-tailed unpaired *t*-tests were performed using GraphPad Prism 5 software. Differences corresponding to *P* values less than 0.05 were considered to be statistically significant.

Results

Differential scanning calorimetry of DHP107 and F109

Heating thermograms of dry and hydrated F109 and DHP107 were obtained between -30°C and 30°C (Figure 1). Dry F109

and DHP107 showed an exotherm with an onset temperature of approximately -25°C and two endotherms with onset temperatures of 4°C and 12°C . The phase transitions of DHP107 had much broader temperature ranges than those of F109, probably because of the presence of paclitaxel as an impurity. The dry formulations became wax at temperatures below 4°C but were partially melted above 4°C and were completely melted above approximately 30°C . For the hydrated samples, ice melting was observed at 0°C , and an endotherm was observed at approximately 5°C . Hydrated DHP107 showed an additional endotherm at approximately 11°C and was completely melted at 15°C .

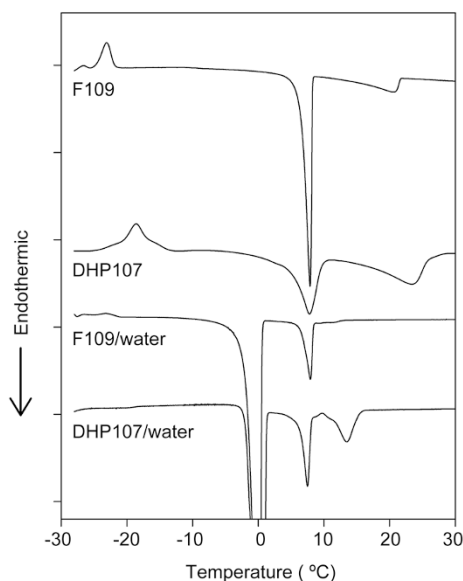


Figure 1. Heating thermograms of dry and hydrated F109 and DHP107.

Small angle X-ray diffraction

SAXS patterns were obtained for F109 and DHP107 in the hydration range of 0% to 50% (*v/v*, Figures 2A and S1). The d-spacing was plotted as a function of water content in Figure 2B; dry F109 was in the fluid isotropic phase with a d-spacing of approximately 32 \AA ($2\theta=2.75$), whereas dry DHP107 revealed coexistence of the fluid isotropic (31 \AA , $2\theta=2.77$) and lamellar phases (49 \AA , $2\theta=1.79$). As the water content of samples increased, the d-spacing increased gradually and plateaued at values of 94 \AA ($2\theta=0.94$) and 85 \AA ($2\theta=1.03$) for F109 and DHP107, respectively, at approximately 33% (*v/v*) hydration. The single broad diffraction at a very low angle in the diffraction patterns of the fully hydrated DHP107 and F109 samples can be interpreted as evidence of the existence of a lipidic sponge phase, or an L_3 phase^[28]. When observed by polarized microscopy, the samples did not show any birefringence, thus indicating the existence of the sponge phase rather than other 1- or 2-dimensional disordered liquid crystalline

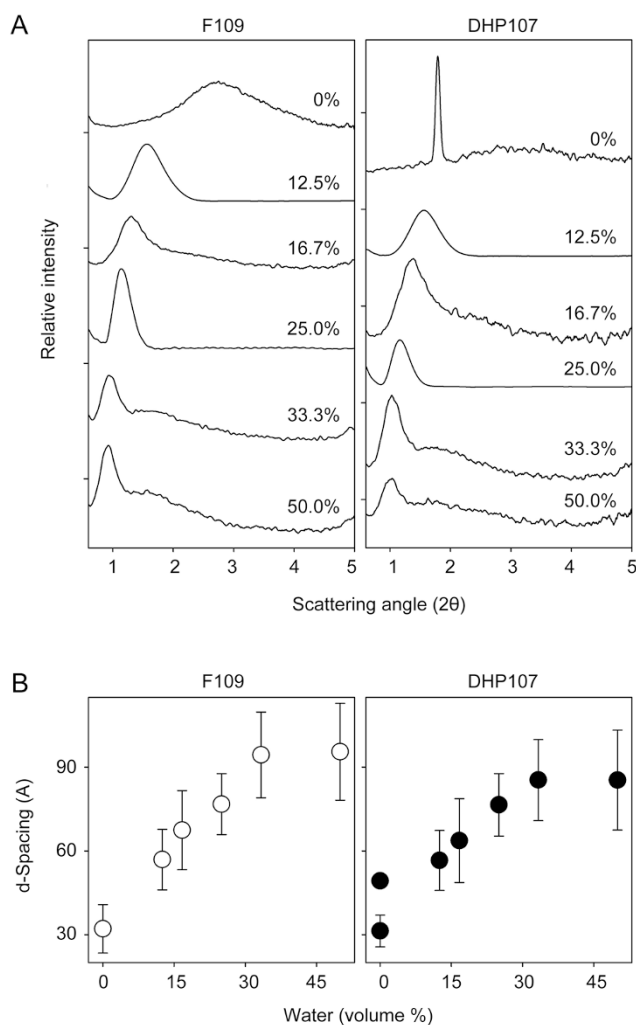


Figure 2. (A) Small-angle X-ray diffraction patterns and (B) d-spacings of F109 and DHP107 at various hydrations.

phases, such as a disordered hexagonal phase.

Cryo-TEM

Hydrated F109 and DHP107 were observed using cryo-TEM at 25% (*v/v*) water in Figure 3. Hydrated F109 showed smoothly curved lamellae with folds, ridges, and grooves in the sponge phase sample. The micrographs of the hydrated DHP107 showed similar structures with folded lamellae but were granulated rather than smooth. Such granulation may represent the crystallization of components such as paclitaxel, owing to the low temperature and may not represent the phase behavior at room temperature. The micrographs of F109 and DHP107 had salient features similar to those of the lipidic sponge phase^[36, 37]. When a sample known to form a lipidic sponge phase was observed, we found highly folded lamellae similar to those of F109 and DHP107. From the results of SAXS and cryo-TEM, we concluded that DHP107 and F109 were likely to form a sponge phase after hydration at room temperature.

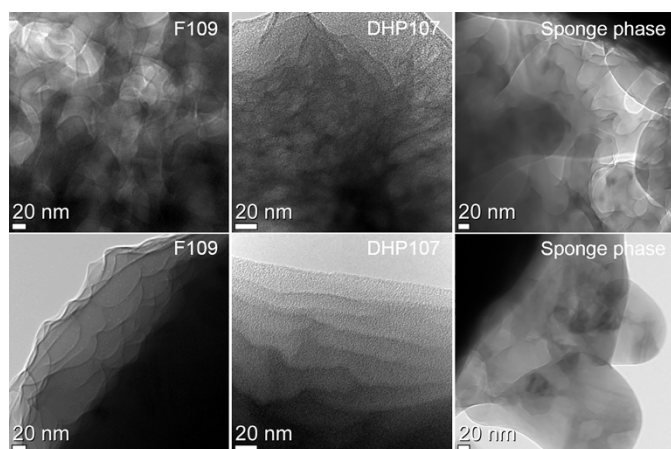


Figure 3. Cryo-transmission electron microscopy micrographs of F109 and DHP107 at 25% (v/v) hydration and the sponge phase sample (PEG400:monoolein:100 mmol/L Tris-HCl=4:3:3, v/v).

A single oral administration of DHP107 under fasted and fed conditions in mice

Plasma paclitaxel concentration-time profiles were evaluated after a single oral administration of 50 mg/kg DHP107 under fasted and fed conditions (Figure 4A). The C_{max} values of the fasted and fed mice were 4.19 $\mu\text{g/mL}$ at 2 h and 3.38 $\mu\text{g/mL}$

at 1 h, respectively. The AUC values for the fasted and fed mice were 13.01 and 15.50 $\mu\text{g h/mL}$, respectively (Table 1). When the mice were in the fed state, the AUC values increased by 19.2%, and smaller C_{max} and T_{max} values than those of the fasted mice were observed.

Oral administration of two DHP107 doses at various time intervals under fasted conditions

To determine how the first oral dose of DHP107 influenced the second dose, the mice were administered DHP107 twice at various dosing intervals under fasted conditions. The plasma concentrations of paclitaxel are shown in Figures 4B and S2. The T_{max} and C_{max} values for the 4-, 8-, and 24-h interval groups were the same as those in the single oral administration group under fasted conditions because the second peak was smaller than the first. The total AUC values for the 2-, 4-, 8-, and 24-h interval groups were 22.19, 14.99, 14.06, and 13.78 $\mu\text{g h/mL}$, respectively, whereas the AUC value for the single dose group was 13.01 $\mu\text{g h/mL}$ (Table 1). These values corresponded to 70.6%, 15.2%, 8.1%, and 5.9% increases, respectively, after the second dose, thus indicating that absorption was highest when the interval between the two doses was 2 h. The C_{max} values of the second dose in the 2-, 4-, 8-, and 24-h interval groups were 7.41 $\mu\text{g/mL}$ at 2.5 h, 1.89 $\mu\text{g/mL}$ at 5 h, 0.74 $\mu\text{g/mL}$ at 9 h, and 0.35 $\mu\text{g/mL}$ at 25 h, respectively. Except for the 2-h interval

Table 1. Calculated plasma pharmacokinetic parameters of paclitaxel after oral administration of DHP107 (50 mg/kg) in the single- and double-dose groups at various dosing intervals under fasted and fed conditions in mice ($n=5-20/\text{time point}$).

Dosing method		Condition (h)	Interval (h)	T_{max}^a (h)	C_{max} ($\mu\text{g/mL}$)	AUC_{inf} ($\mu\text{g h/mL}$)	
DHP107	Single dose	Fasted	–	2	4.19	13.01	
		Fed	–	1	3.38	15.50	
DHP107+DHP107	Total dose	Fasted	2	2.5	7.41	22.19	
			4	2	4.19	14.99	
			8	2	4.19	14.06	
			24	2	4.19	13.78	
			Fed	24	1	3.38	16.46
				48	1	3.38	20.15
	Second dose	Fasted	96	1	3.38	23.38	
			2	2.5 (0.5)	7.41	9.18	
			4	5 (1)	1.89	1.98	
			8	9 (1)	0.74	1.05	
			24	25 (1)	0.35	0.77	
			Fed	24	26 (2)	0.42	0.96
48	49 (1)	1.43		4.65			
96	98 (2)	1.64	7.88				
F109+DHP107	Second dose	Fasted	2	4 (2)	2.63	10.03	
			4	5 (1)	1.80	7.78	
			8	10 (2)	1.61	5.69	
			24	26 (2)	0.50	1.67	
			Fed	24	28 (4)	2.32	9.81
				48	50 (2)	3.06	8.49
96	98 (2)	2.02	8.55				

^a Numbers in parentheses refer to the T_{max} of the second dose.

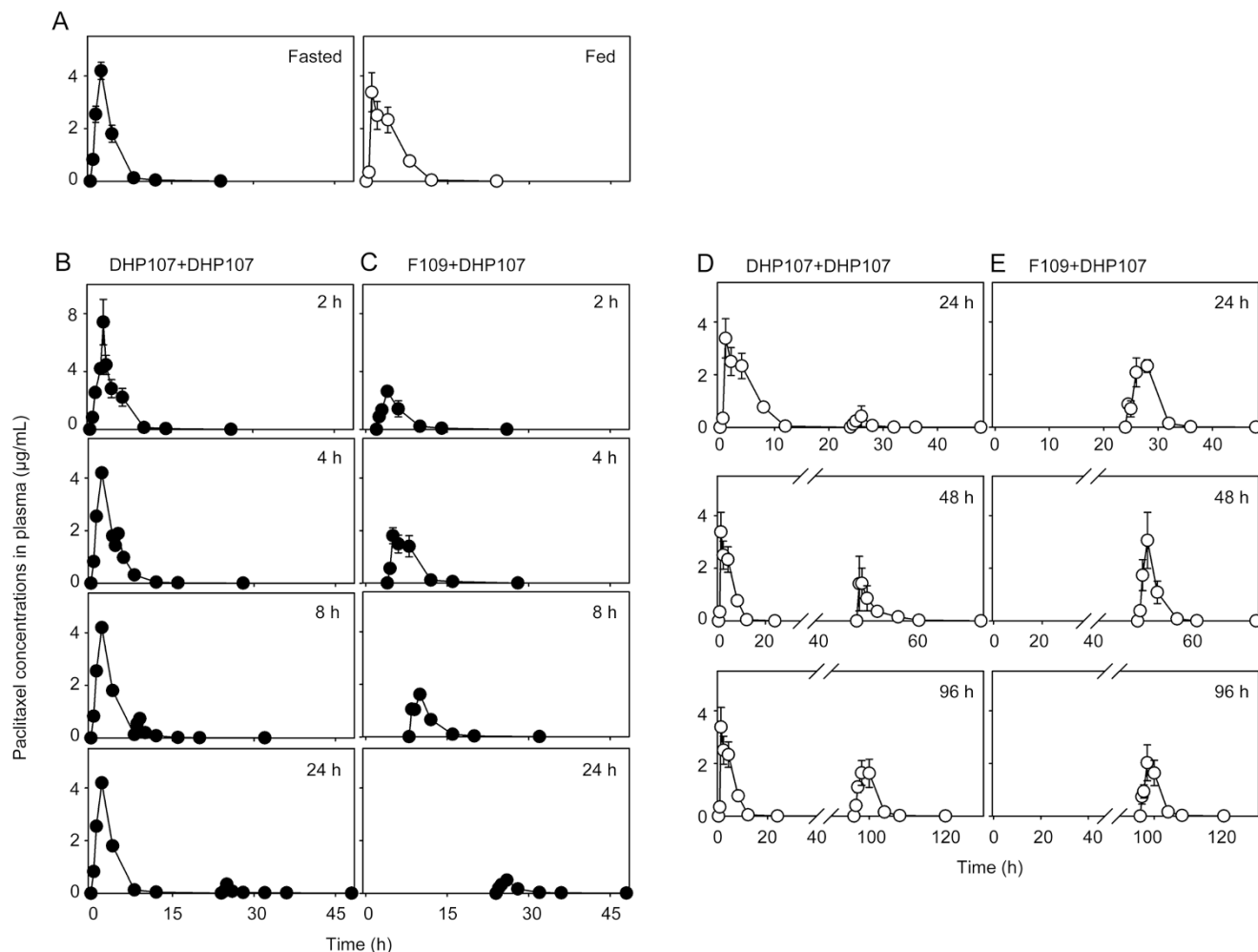


Figure 4. Paclitaxel concentrations in the plasma after oral administration of (A) a single dose of DHP107, (B, D) an initial dose of DHP107 followed by a second dose of DHP107, and (C, E) an initial dose of F109 followed by a second dose of DHP107 at 2-, 4-, 8-, 24-, 48-, and 96-h intervals ($n=5-20$ /time point). DHP107 was administered at 50 mg/kg, and F109 was administered at 5 mL/kg to mice under fasted (B, C, closed circles) and fed (D, E, open circles) conditions.

group, for which there was no separate peak for the second dose, the T_{max} of the second dose occurred at 1 h after the second dose. The AUC values of the second dose of DHP107 were calculated by subtracting the value of the first dose from the total AUC. The AUC values of the second dose in the 2-, 4-, 8-, and 24-h interval groups were 9.18, 1.98, 1.05, and 0.77 $\mu\text{g}\cdot\text{h}/\text{mL}$, respectively (Table 1). All AUC values after double dosing were smaller than those after single dosing and decreased with increasing time intervals. The T_{max} of the second dose was 1 h, whereas that of the first dose was 2 h in the fasted group.

Oral administration of F109 followed by DHP107 under fasted conditions

To observe how F109 altered the absorption of paclitaxel, F109 was administered as the first dose before DHP107 at the various dosing intervals (Figures 4C and S2). The volume of F109

was 5 mL/kg, which was the same volume as that of DHP107 at a dose of 50 mg/kg. The C_{max} values of the second dose of DHP107 in the 2-, 4-, 8-, and 24-h interval groups were 2.63 $\mu\text{g}/\text{mL}$ at 4 h, 1.80 $\mu\text{g}/\text{mL}$ at 5 h, 1.61 $\mu\text{g}/\text{mL}$ at 10 h, and 0.50 $\mu\text{g}/\text{mL}$ at 26 h, respectively. The AUC values for the 2-, 4-, 8-, and 24-h interval groups were 10.03, 7.78, 5.69, and 1.67 $\mu\text{g}\cdot\text{h}/\text{mL}$, respectively, corresponding to 77.1%, 59.8%, 43.7%, and 12.8% of the single DHP107 dose (Table 1). The C_{max} and AUC values decreased with longer time intervals, similarly to the results of the double DHP107 dosing experiment presented above. Thus, when F109 was administered as the first dose instead of DHP107, the AUCs for the second dose of DHP107 were 1.1, 3.9, 5.4, and 2.2 times higher for the 2-, 4-, 8-, and 24-h interval groups, respectively, in the fasted mice (Figures 4B and 4C). These results indicated that the initial administration of paclitaxel blocked the absorption of the subsequent dose of paclitaxel.

Recovery of paclitaxel absorption in the second dose after food intake

The absorption of paclitaxel after a single oral dose of DHP107 differed according to the food intake of the mice, as shown above. Although the increase in the AUC was only approximately 20% when the mice were fed compared with when they were fasted, we repeatedly observed this difference^[1]. Moreover, the T_{\max} value in the fed group was 1 h, whereas that in the fasted group was 2 h, thus indicating that food in the gastrointestinal tract influenced drug absorption. Consequently, we administered two oral doses of DHP107 at various intervals from 2 to 24 h under the fed condition. To observe how the absorption changed when the mice were fed throughout the experiment, mice were administered DHP107 (Figure 4D) or F109 (Figure 4E) followed by a second dose of DHP107 at 24-, 48-, or 96-h intervals and were given free access to food. The C_{\max} values for the second dose of DHP107 were 0.42 $\mu\text{g}/\text{mL}$ at 26 h, 1.43 $\mu\text{g}/\text{mL}$ at 49 h, and 1.64 $\mu\text{g}/\text{mL}$ at 98 h, and the total AUCs for DHP107 in the fed mice were 16.46, 20.15, and 23.38 $\mu\text{g}\cdot\text{h}/\text{mL}$ in the 24-, 48-, and 96-h interval groups, respectively. The AUC values changed dramatically when the time interval increased. The AUC values of the second dose were 0.96, 4.65, and 7.88 $\mu\text{g}\cdot\text{h}/\text{mL}$ in the 24-, 48-, and 96-h interval groups, respectively, corresponding to 6.2%, 30%, and 50.9%, respectively, of the single-dose AUC under the fed conditions (Table 1). When F109 (5 mL/kg) was orally administered to the fed mice instead of DHP107 as the first dose, the C_{\max} values in the 24-, 48-, and 96-h interval groups were 2.32 $\mu\text{g}/\text{mL}$ at 28 h, 3.06 $\mu\text{g}/\text{mL}$ at 50 h, and 2.02 $\mu\text{g}/\text{mL}$ at 98 h, respectively (Figure 4E). The AUC values in the 24-, 48-, and 96-h interval groups were 9.81, 8.49, and 8.55 $\mu\text{g}\cdot\text{h}/\text{mL}$, respectively (Table 1). Thus, when F109 was administered as the first dose instead of DHP107, the AUCs for the second dose of DHP107 were 10.2, 1.8, and 1.1 times higher for the 24-, 48-, and 96-h interval groups, respectively, in the fed mice (Figures 4D and 4E). Similarly to the findings in the fasted mice, the initial dose of paclitaxel inhibited the absorption of the subsequent paclitaxel dose in the fed mice.

Western blotting

In the experiments described above, the AUC values for the second oral DHP107 dose were consistently smaller than those of the first dose. A decrease in paclitaxel absorption after repeated dosing has also been reported in previous studies^[20, 25–27]. Moreover, paclitaxel is known to be a substrate of P-gp and is metabolized mainly by CYP3A4 and CYP2C8, and increased P-gp and CYP expression after oral paclitaxel administration has been demonstrated and confirmed by observations that paclitaxel absorption increases after co-administration with P-gp inhibitors^[25–27]. To evaluate whether the expression levels of P-gp, CYP3A4, and CYP2C8 were enhanced by oral paclitaxel administration, we performed Western blot analysis of these proteins in the livers and small intestines of mice collected up to 7 d after a single dose of oral DHP107 at 50 mg/kg (Figure 5). P-gp, CYP3A4, and CYP2C8 were detected as 170-, 50-, and 56-kDa bands,

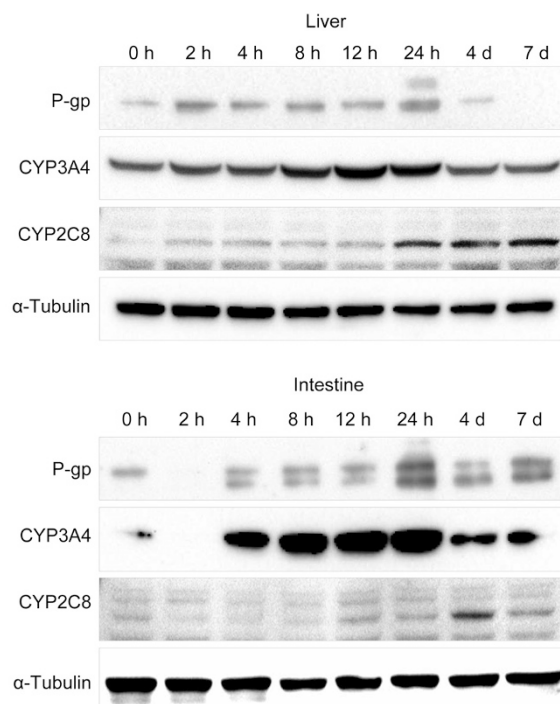


Figure 5. Expression of P-glycoprotein (P-gp), CYP3A4, and CYP2C8, as analyzed by Western blotting, in liver and small intestine homogenates at different time points after oral administration of DHP107 at a dose of 50 mg/kg in mice ($n=3/\text{time point}$).

respectively. P-gp and CYP proteins are typically detected as double bands and single bands in the small intestine, respectively^[29]. P-gp expression gradually increased, peaking at 24 h in both the liver and the small intestine. CYP3A4 also gradually increased, peaking at 12–24 h and then subsequently decreasing. CYP2C8 expression increased slowly and did not decrease during the duration of the experiment. The time-dependent intensity profiles of the CYP3A4 bands were similar to those of P-gp but differed from those of CYP2C8. The results showed that the absorption of paclitaxel measured from 2 h to 7 d after the previous dose was inhibited by P-gp and CYPs and that the inhibition was highest when the dosing interval was 24 h.

Mucoadhesiveness

Although increased P-gp and CYP expression may have explained the decreased absorption of paclitaxel when DHP107 was administered twice, it was unclear why absorption decreased when F109, a formulation without paclitaxel, was administered as the first dose. As shown above, our DHP107 and F109 formulations were in the lipidic sponge phase upon hydration (Figures 2 and 3). The sponge phase is viscous^[28, 36, 37], although much less viscous than the cubic phase of hydrated monoolein, which is known to be mucoadhesive^[38]. The mucoadhesiveness of DHP107 has also been demonstrated by adsorption to the intestinal wall^[2]. Therefore, we attempted to quantify the mucoadhesiveness of F109

compared with that of hydrated monoolein by performing an *ex vivo* everted sac experiment. Other components and their combinations in DHP107 were also studied, and Taxol[®] was used as a control. Oil red O, a red-colored probe, was used to analyze and quantify the formulation adherence on the everted sac (Figure 6). Mucoadhesiveness, quantified as the weight of the adhered formulation in the unit area, was highest for the monoolein and monoolein/polysorbate 80 systems. The amount of adhered F109 was approximately 60% and 40% that of monoolein and monoolein/polysorbate 80, respectively. In the case of Taxol[®], the red color of oil red O appeared to have stained the tissue, owing to the presence of ethanol in the Taxol[®] formulation rather than to the adherence of Taxol[®]. Although monoolein/polysorbate 80 had the strongest mucoadhesiveness among the formulations, mucoadhesiveness was considerably lower for the monoolein/tricaprylin system. Together, these results suggested that the mucoadhesiveness of F109 was approximately half that of monoolein.

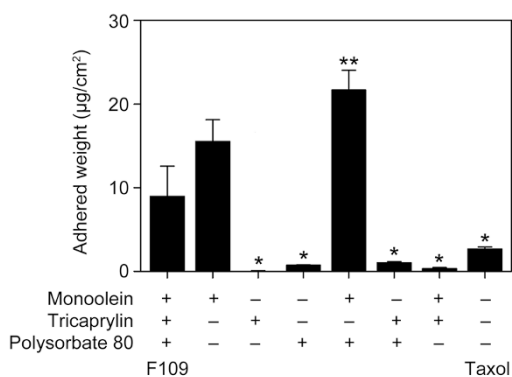


Figure 6. Weight of the adhered formulation per unit area on everted sacs after treatment with F109, combinations of the components, and Taxol[®] containing oil red O at 37 °C ($n=6/\text{group}$). * $P<0.05$, ** $P<0.01$ compared with F109.

Observation of F109 in the intestinal lumen

An F109-containing Nile red probe was administered orally to mice at 5 µL/kg to observe the upper intestine at 2 and 24 h after administration (Figure 7). In our previous study, we have observed the interaction of DHP107 with the intestinal fluid in the intestine at various time points in fasted mice^[2]. In this study, experiments were carried out in both fed and fasted mice. Well-defined oil droplets with diameters of approximately 10 µm were observed on the surface of the lumen at 2 h in the fasted mice. In the fed mice, droplets existed in turbid solution at 2 h. When the lumen was observed at 24 h, turbid samples remained in the fasted group but were almost completely absent in the fed group.

Effects of bile excretion on the absorption of oral DHP107

DHP107 is a formulation composed of oils. When oil is taken orally, bile is excreted and subsequently aids in digestion by facilitating micellization of the oil. DHP107 contains 27.5%

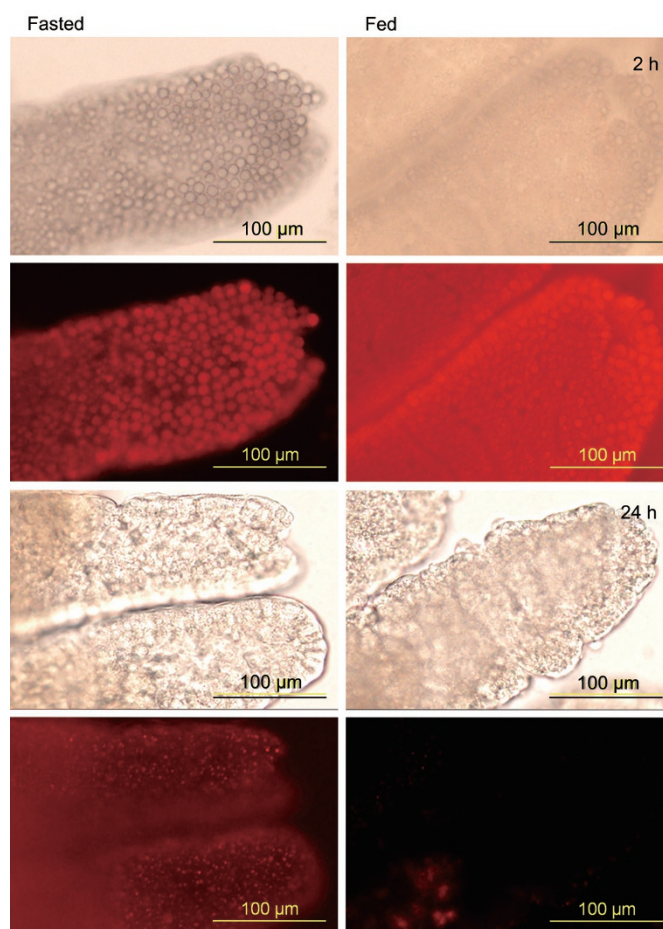


Figure 7. Optical and fluorescence photomicrographs of the intestinal lumen at 2 and 24 h after oral administration of F109 containing Nile red at a dose of 5 mL/kg under fasted and fed conditions ($n=3/\text{group}$).

(*w/w*) tricaprilyn, which can be digested by lipase in the intestine. Bile excretion, therefore, may be an important factor that affects the absorption of paclitaxel in DHP107. If bile were depleted after the first dose, it might not be sufficiently replenished for emulsification of the formulation in the second dose, thus causing decreased paclitaxel absorption.

To evaluate how bile influences the absorption of oral DHP107, we performed two sets of experiments (Figure 8). First, bile was orally administered along with DHP107 to rats without gall bladders^[39] to mimic the burst excretion of bile. Then, in a second experiment, cholecystectomies were performed in mice to remove the source of burst bile excretion. There were no significant differences in AUC values with or without bile in rats (Figure 8A). In the case of mice, paclitaxel absorption from DHP107 was virtually identical in the cholecystectomy model and the sham-operated control (Figure 8B). From these experiments, we concluded that the absorption of paclitaxel in DHP107 was not influenced by bile.

Discussion

In this study, we examined the phases of DHP107 in water and

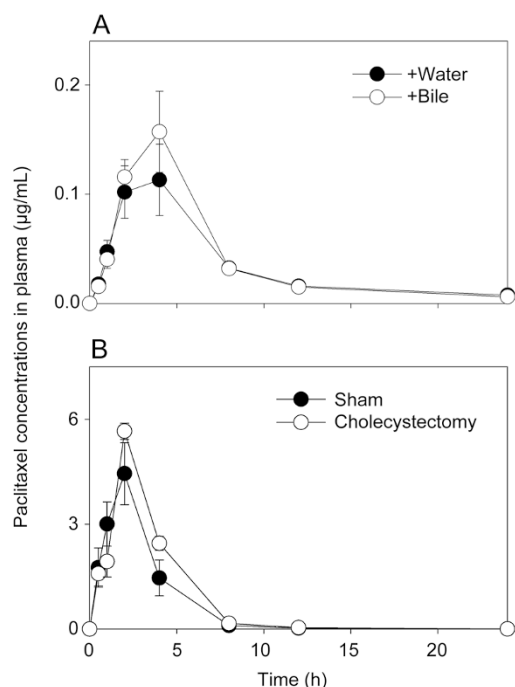


Figure 8. Paclitaxel concentrations in the plasma after oral administration of DHP107 (A) followed by administration of water or rat bile (5 mL/kg) at 1 min in rats (25 mg/kg, $n=10$ /group) and (B) in the mouse cholecystectomy model (50 mg/kg, $n=5$ /time point).

evaluated the pharmacokinetics and absorption of paclitaxel in DHP107 in mice and rats. Our results demonstrated that the bioavailability of DHP107 is enhanced through its mucoadhesive properties and that DHP107 absorption can be altered by the dosing interval and food intake, without being affected by bile. These findings provide important insight into the appropriate dosing regimen of DHP107.

DHP107 is an oily formulation that melts completely at approximately 30°C (Figure 1), undergoes an exothermic transition at approximately -20°C, and remains as a single solid phase up to 0°C. As the temperature increases from 0°C to 30°C, tricaprylin begins to melt at 4°C, followed by monoolein at 12°C; monoolein and tricaprylin then becomes immiscible in the temperature range from 4 to 30°C^[1]. However, after melting above 30°C, DHP107 forms a single liquid phase without phase separation. Once melted, this formulation can be super-cooled and can remain in liquid form at room temperature for up to several hours. Moreover, our data demonstrated ice melting in hydrated DHP107, and two additional endotherms could be similarly assigned to the dry DHP107 system. Dry or hydrated F109 showed behaviors similar to those of DHP107.

Previously, we have reported that DHP107 is mucoadhesive, although we did not evaluate the nature of the mucoadhesiveness^[2]. Because DHP107 contains 55% (*w/w*) monoolein, we predicted the formation of a highly viscous cubic phase in water or the intestine^[38]. The driving force for the formation of the cubic phase in hydrated monoolein comes from the tendency of monoolein to curl away from the planar lamel-

lar phase. This tendency can be expressed as the curvature elastic energy function^[40, 41]. Our findings, however, demonstrated that DHP107 did not form a cubic phase. From SAXS and cryo-TEM experiments, we found that DHP107 formed a sponge phase, that is, a disordered analog of the cubic phase. The sponge phase was less viscous than the cubic phase but retained approximately half the mucoadhesiveness of the cubic phase, thus increasing the bioavailability of oral DHP107 by allowing it to adhere to the mucous layer in the intestine where absorption effectively occurred.

In this study, we found that when DHP107 was administered twice at various dosing intervals, the AUC values after the second dose of DHP107 were lower than those of the first dose of DHP107. We propose three major reasons for this outcome. First, the expression levels of P-gp and CYPs may have increased after the first dose of DHP107. Second, mucoadhesive F109 may have persisted on the mucous layer and prohibited the adhesion of the formulation in the second dose. Third, reduced excretion of bile for the second dose may have resulted in less efficient micellization of DHP107 for oil digestion and uptake. These three possibilities were explored in our study, as discussed below.

Paclitaxel has a low oral bioavailability, owing to the multidrug efflux pump P-gp in the intestine and to hepatic and intestinal first-pass elimination by CYPs^[25-27]. In this study, we evaluated the effects of P-gp and CYPs by administering F109 instead of DHP107 as the first dose. Because the formulation of F109 is identical to that of DHP107, except for the presence of paclitaxel, and because F109 has physical properties similar to those of DHP107, this experiment was expected to provide insight into the effects of paclitaxel in the first DHP107 dose on the absorption of paclitaxel in the subsequent dose. The results showed that the differences in the AUC values increased when the time interval increased and was highest when the time interval was 24 h but decreased with longer time intervals. Moreover, paclitaxel absorption from the second DHP107 dose was approximately 1-10 times higher when F109 was administered instead of DHP107 as the first dose. This result was consistent with the expression of proteins responsible for drug efflux and metabolism, as evaluated by a Western blot analysis; the expression levels of P-gp and CYP3A4 were highest 24 h after administration of DHP107.

In our analysis of the mucoadhesiveness of the formulation, we found that DHP107 adhered to the mucous layer of the intestine and that most DHP107 absorption was complete within 8 h of administration in mice, consistently with the results of previous studies^[1, 2, 7]. Adherence of the formulation to the intestine might subsequently prohibit the adsorption of DHP107 administered in the second dose and therefore lower the absorption of paclitaxel. To test this possibility, we performed pharmacokinetic studies in fasted and fed animals and found that the presence of food aided in dispersing DHP107 and shortened the T_{max} from 2 h in the fasted group to 1 h in the fed group. Increased gastrointestinal motility stimulated by food may help solubilize paclitaxel and stabilize microemulsified droplets in the formulation. The

absorption of drugs that have poor aqueous solubility can be increased by food intake. For example, the absorption of itraconazole, which has poor aqueous solubility, is increased by food intake^[42]. Food intake may facilitate the solubilization of lipophilic paclitaxel and enhance the absorption of paclitaxel in the gastrointestinal tract, because the solubilizing step is likely to be the rate-determining step during the absorption of poorly soluble drugs. Bile excretion is also stimulated by food and can increase the solubilization of the adhered formulation to the intestinal wall. However, bile did not affect the absorption of DHP107 in our study. As the second dose of DHP107 enters the intestine, food particles and increased gastrointestinal motility caused by food intake may facilitate the removal of the adhered formulation, which would have already released paclitaxel from the intestinal mucus, thereby preparing the intestine for the next dose for adhesion. Notably, the AUC value was much higher in the fed mice than in the fasted mice when F109, rather than DHP107, was administered as the first dose in the 24-h interval group. Although the increase in AUC could also be explained by other factors when DHP107 was administered twice, these effects might have primarily been due to the active removal of F109 by food, thus allowing DHP107 to adhere when F109 was administered as the first dose. Indeed, we found that food in the intestine facilitated the dispersion of DHP107 within 2 h and enhanced the removal of the remaining DHP107 from the intestinal wall by 24 h. This result further indicates that DHP107 is indeed a mucoadhesive drug delivery system. The mucoadhesiveness of DHP107 was found to be approximately 60% that of monoolein, as shown in *ex vivo* experiments using the everted sac method.

Finally, we examined whether bile affected the absorption of the second dose of DHP107. When oil enters the gastrointestinal tract, bile is excreted to aid in the digestion process^[43]. Large amounts of bile may be excreted through the bile duct when relatively large amounts of triglycerides enter the system. Notably, rats do not have a gallbladder^[39] and do not excrete high concentrations of bile in the presence of fats and oils in the gastrointestinal tract, but instead exhibit continuous secretion of bile at a low concentration^[39,44]. Therefore, in rats, we administered bile along with DHP107 to determine the effects of bile on drug absorption. Additionally, we used a cholecystectomy model in mice to further examine the effects of bile. Interestingly, in both models, bile had no effect on the absorption of DHP107.

DHP107 is a mucoadhesive oral formulation of paclitaxel whose absorption is influenced by P-gp and CYPs. Thus, the dosing schedule of DHP107 may be important for maximizing drug absorption. The administration of a second dose of DHP107 before P-gp and CYP levels are increased may be an efficient dosing method. In mice, a 2-h interval yielded the highest AUC. Moreover, food intake is also important. DHP107 was more efficiently absorbed in fed conditions than in fasted conditions for both the single-dose and double-dose schedules. Finally, bile did not affect the absorption of DHP107. These findings may provide insight into the appro-

priate DHP107 dosing schedule for patients with cancer.

Conclusion

In summary, we showed that DHP107 is a mucoadhesive formulation that forms a lipidic sponge phase upon hydration. We elucidated the absorption mechanism of DHP107 and optimized the treatment schedule for two oral doses of DHP107. The recommended dosing interval for oral DHP107 administration is less than 4 h or more than 24 h, to avoid the highest expression of P-gp and CYPs in mice. Additionally, the absorption of DHP107 was higher when administered to mice during normal food intake and was unaffected by bile. Therefore, in clinical studies, it is expected that patients with impaired gallbladder function may also benefit from treatment with DHP107. Moreover, when using a b.i.d. dosing regimen, the interval between doses may be an important factor in achieving the maximum absorption of paclitaxel from DHP107 in patients.

Further studies are being undertaken to analyze the distribution of paclitaxel in various tissues, including lymph and tumor tissues, to further understand the detailed absorption mechanism of paclitaxel in DHP107 and to improve the formulation by increasing the oral bioavailability while minimizing formulation-related side-effects.

Acknowledgements

This study was supported by an intramural grant from the Korea Institute of Science and Technology (No 2E24670) and a grant from the Korea Evaluation Institute of Industrial Technology (No 10044731).

Author contribution

Yura JANG, Jung Wan HONG, and Hesson CHUNG designed the study; Yura JANG, Jung Wan HONG, Cheol-Won YUN, Hye Jin CHUNG, and Hesson CHUNG performed the research; Yura JANG, Hye Jin CHUNG, and Hesson CHUNG analyzed the data and wrote the paper.

Supplementary information

Supplementary information is available on Acta Pharmacologica Sinica's web site.

References

- 1 Lee IH, Hong JW, Jang Y, Park YT, Chung H. Development, optimization and absorption mechanism of DHP107, oral paclitaxel formulation for single-agent anticancer therapy. In: Thomas B, editor. New advances in the basic and clinical gastroenterology. Croatia: InTech; 2012. p 357–74.
- 2 Hong JW, Lee IH, Kwak YH, Park YT, Sung HC, Kwon IC, et al. Efficacy and tissue distribution of DHP107, an oral paclitaxel formulation. Mol Cancer Ther 2007; 6: 3239–47.
- 3 Han J, Chung H, Lee JH, Suh JE, Lee GS, Kim JC, et al. Single and two-week repeated oral dose toxicity study of DHP2, a hydrophobic drug delivery vehicle in mice. Toxicol Res 2004; 20: 123–9.
- 4 Lee SJ, Kim SW, Chung H, Park YT, Choi YW, Cho YH, et al. Bioadhesive drug delivery system using glyceryl monooleate for the intravesical administration of paclitaxel. Chemotherapy 2005; 51:

- 311–8.
- 5 Choe HS, Kim SW, Cho YH. Anticancer activity of intravesical glyceryl monooleate (GMO)-paclitaxel therapy in murine superficial transitional cell carcinoma model induced by BBN. *Korean J Urol* 2006; 47: 1155–60.
 - 6 Kim DB, Jang J, Cho YH, Yoon MS, Chung H, Park YT, et al. Anticancer efficacy and toxicity of oral GMO-paclitaxel in a hormone refractory prostate cancer model. *Korean J Urol* 2006; 47: 143–9.
 - 7 Shin BS, Kim HJ, Hong SH, Lee JB, Hwang SW, Lee MH, et al. Enhanced absorption and tissue distribution of paclitaxel following oral administration of DHP 107, a novel mucoadhesive lipid dosage form. *Cancer Chemother Pharmacol* 2009; 64: 87–94.
 - 8 Ho PY, Yeh TK, Yao HT, Lin HL, Wu HY, Lo YK, et al. Enhanced oral bioavailability of paclitaxel by *D*-alpha-tocopheryl polyethylene glycol 400 succinate in mice. *Int J Pharm* 2008; 359: 174–81.
 - 9 Kim SC, Kim DW, Shim YH, Bang JS, Oh HS, Wan Kim S, et al. *In vivo* evaluation of polymeric micellar paclitaxel formulation: toxicity and efficacy. *J Control Release* 2001; 72: 191–202.
 - 10 Foger F, Malaivijitnond S, Wannaprasert T, Huck C, Bernkop-Schnurch A, Werle M. Effect of a thiolated polymer on oral paclitaxel absorption and tumor growth in rats. *J Drug Target* 2008; 16: 149–55.
 - 11 Lee E, Lee J, Lee IH, Yu M, Kim H, Chae SY, et al. Conjugated chitosan as a novel platform for oral delivery of paclitaxel. *J Med Chem* 2008; 51: 6442–9.
 - 12 Nornoo AO, Zheng H, Lopes LB, Johnson-Restrepo B, Kannan K, Reed R. Oral microemulsions of paclitaxel: *in situ* and pharmacokinetic studies. *Eur J Pharm Biopharm* 2009; 71: 310–7.
 - 13 Ganta S, Devalapally H, Amiji M. Curcumin enhances oral bioavailability and anti-tumor therapeutic efficacy of paclitaxel upon administration in nanoemulsion formulation. *J Pharm Sci* 2010; 99: 4630–41.
 - 14 Jin J, Bi H, Hu J, Zhong G, Zhao L, Huang Z, et al. Enhancement of oral bioavailability of paclitaxel after oral administration of Schisandrol B in rats. *Biopharm Drug Dispos* 2010; 31: 264–8.
 - 15 Zhao L, Feng SS. Enhanced oral bioavailability of paclitaxel formulated in vitamin E-TPGS emulsified nanoparticles of biodegradable polymers: *in vitro* and *in vivo* studies. *J Pharm Sci* 2010; 99: 3552–60.
 - 16 Iqbal J, Sarti F, Perera G, Bernkop-Schnurch A. Development and *in vivo* evaluation of an oral drug delivery system for paclitaxel. *Biomaterials* 2011; 32: 170–5.
 - 17 Mo R, Jin X, Li N, Ju C, Sun M, Zhang C, et al. The mechanism of enhancement on oral absorption of paclitaxel by *N*-octyl-*O*-sulfate chitosan micelles. *Biomaterials* 2011; 32: 4609–20.
 - 18 Pandita D, Ahuja A, Lather V, Benjamin B, Dutta T, Velpandian T, et al. Development of lipid-based nanoparticles for enhancing the oral bioavailability of paclitaxel. *AAPS PharmSciTech* 2011; 12: 712–22.
 - 19 Flores JP, Saif MW. Novel oral taxane therapies: recent phase I results. *Clin Investig (Lond)* 2013; 3: 333–41.
 - 20 Hahn HS, Lee KH, Lee IH, Lee JH, Whang CS, Jo YW, et al. Metronomic oral paclitaxel shows anti-tumor effects in an orthotopic mouse model of ovarian cancer. *J Gynecol Oncol* 2014; 25: 130–5.
 - 21 Hong YS, Kim KP, Lim HS, Bae KS, Ryu MH, Lee JL, et al. A phase I study of DHP107, a mucoadhesive lipid form of oral paclitaxel, in patients with advanced solid tumors: crossover comparisons with intravenous paclitaxel. *Invest New Drugs* 2013; 31: 616–22.
 - 22 Lim HS, Bae KS, Jung JA, Noh YH, Hwang AK, Jo YW, et al. Predicting the efficacy of an oral paclitaxel formulation (DHP107) through modeling and simulation. *Clin Ther* 2015; 37: 402–17.
 - 23 Ryu MH, Ryoo BY, Kim TW, Kim SB, Lim HS, Bae KS, et al. A phase I/II study of DHP107, a novel oral paclitaxel formulation, in patients with advanced solid tumors (phase I) and gastric cancer (phase II). *J Clin Oncol* 2014; 32: abstr 101.
 - 24 Kang YK, Ryu MH, Park SR, Kim JG, Kim JW, et al. Efficacy and safety findings from DREAM: A phase III study of DHP107 (oral paclitaxel) vs IV paclitaxel in patients with gastric cancer after failure of first-line chemotherapy. *J Clin Oncol* 2016; 34 Suppl: 4016.
 - 25 Malingre MM, Beijnen JH, Rosing H, Koopman FJ, van Tellingen O, Duchin K, et al. A phase I and pharmacokinetic study of bi-daily dosing of oral paclitaxel in combination with cyclosporin A. *Cancer Chemother Pharmacol* 2001; 47: 347–54.
 - 26 Kruijtzter CM, Schellens JH, Mezger J, Scheulen ME, Keilholz U, Beijnen JH, et al. Phase II and pharmacologic study of weekly oral paclitaxel plus cyclosporine in patients with advanced non-small-cell lung cancer. *J Clin Oncol* 2002; 20: 4508–16.
 - 27 Kruijtzter CM, Boot H, Beijnen JH, Lochs HL, Parnis FX, Planting AS, et al. Weekly oral paclitaxel as first-line treatment in patients with advanced gastric cancer. *Ann Oncol* 2003; 14: 197–204.
 - 28 Wohri AB, Johansson LC, Wadsten-Hindrichsen P, Wahlgren WY, Fischer G, Horsefield R, et al. A lipidic-sponge phase screen for membrane protein crystallization. *Structure* 2008; 16: 1003–9.
 - 29 Matheny CJ, Ali RY, Yang X, Pollack GM. Effect of prototypical inducing agents on P-glycoprotein and CYP3A expression in mouse tissues. *Drug Metab Dispos* 2004; 32: 1008–14.
 - 30 Tonsberg H, Holm R, Bjerregaard TG, Boll JB, Jacobsen J, Mullertz A. An updated and simplified method for bile duct cannulation of rats. *Lab Anim* 2010; 44: 373–6.
 - 31 Ibrahim A, Gilzad-kohan MH, Aghazadeh-Habashi A, Jamali F. Absorption and bioavailability of glucosamine in the rat. *J Pharm Sci* 2012; 101: 2574–83.
 - 32 Amigo L, Husche C, Zanlungo S, Lutjohann D, Arrese M, Miquel JF, et al. Cholecystectomy increases hepatic triglyceride content and very-low-density lipoproteins production in mice. *Liver Int* 2011; 31: 52–64.
 - 33 Liu A, Lou H, Zhao L, Fan P. Validated LC/MS/MS assay for curcumin and tetrahydrocurcumin in rat plasma and application to pharmacokinetic study of phospholipid complex of curcumin. *J Pharm Biomed Anal* 2006; 40: 720–7.
 - 34 Santos CA, Jacob JS, Hertzog BA, Freedman BD, Press DL, Harnpicharnchai P, et al. Correlation of two bioadhesion assays: the everted sac technique and the CAHN microbalance. *J Control Release* 1999; 61: 113–22.
 - 35 Jonganurakkun B, Liu XD, Nodasaka Y, Nomizu M, Nishi N. Survival of lactic acid bacteria in simulated gastrointestinal juice protected by a DNA-based complex gel. *J Biomater Sci Polym Ed* 2003; 14: 1269–81.
 - 36 Wolf L, Hoffmann H, Talmon Y, Teshigawara T, Watanabe K. Cryo-TEM imaging of a novel microemulsion system of silicone oil with an anionic/nonionic surfactant mixture. *Soft Matter* 2010; 6: 5367–74.
 - 37 Danino D, Weihs D, Zana R, Oradd G, Lindblom G, Abe M, et al. Microstructures in the aqueous solutions of a hybrid anionic fluorocarbon/hydrocarbon surfactant. *J Colloid Interface Sci* 2003; 259: 382–90.
 - 38 Ganem-Quintanar A, Quintanar-Guerrero D, Buri P. Monolein: a review of the pharmaceutical applications. *Drug Dev Ind Pharm* 2000; 26: 809–20.
 - 39 Kocsar LT, Bertok L, Varteresz V. Effect of bile acids on the intestinal absorption of endotoxin in rats. *J Bacteriol* 1969; 100: 220–3.
 - 40 Vacklin H, Khoo B, Madan K, Seddon J, Templer R. The bending elasticity of 1-monolein upon relief of packing stress. *Langmuir* 2000; 16: 4741–8.
 - 41 Chung H, Caffrey M. The curvature elastic-energy function of the lipid-water cubic mesophase. *Nature* 1994; 368: 224–6.

- 42 Van Peer A, Woestenborghs R, Heykants J, Gasparini R, Gauwenbergh G. The effects of food and dose on the oral systemic availability of itraconazole in healthy subjects. *Eur J Clin Pharmacol* 1989; 36: 423-6.
- 43 Armand M, Pasquier B, Andre M, Borel P, Senft M, Peyrot J, *et al*. Digestion and absorption of 2 fat emulsions with different droplet sizes in the human digestive tract. *Am J Clin Nutr* 1999; 70: 1096-106.
- 44 Krondl A, Vavrinkova H, Michalec C. Effect of cholecystectomy on the role of the gallbladder in fat absorption. *Gut* 1964; 5: 607-10.